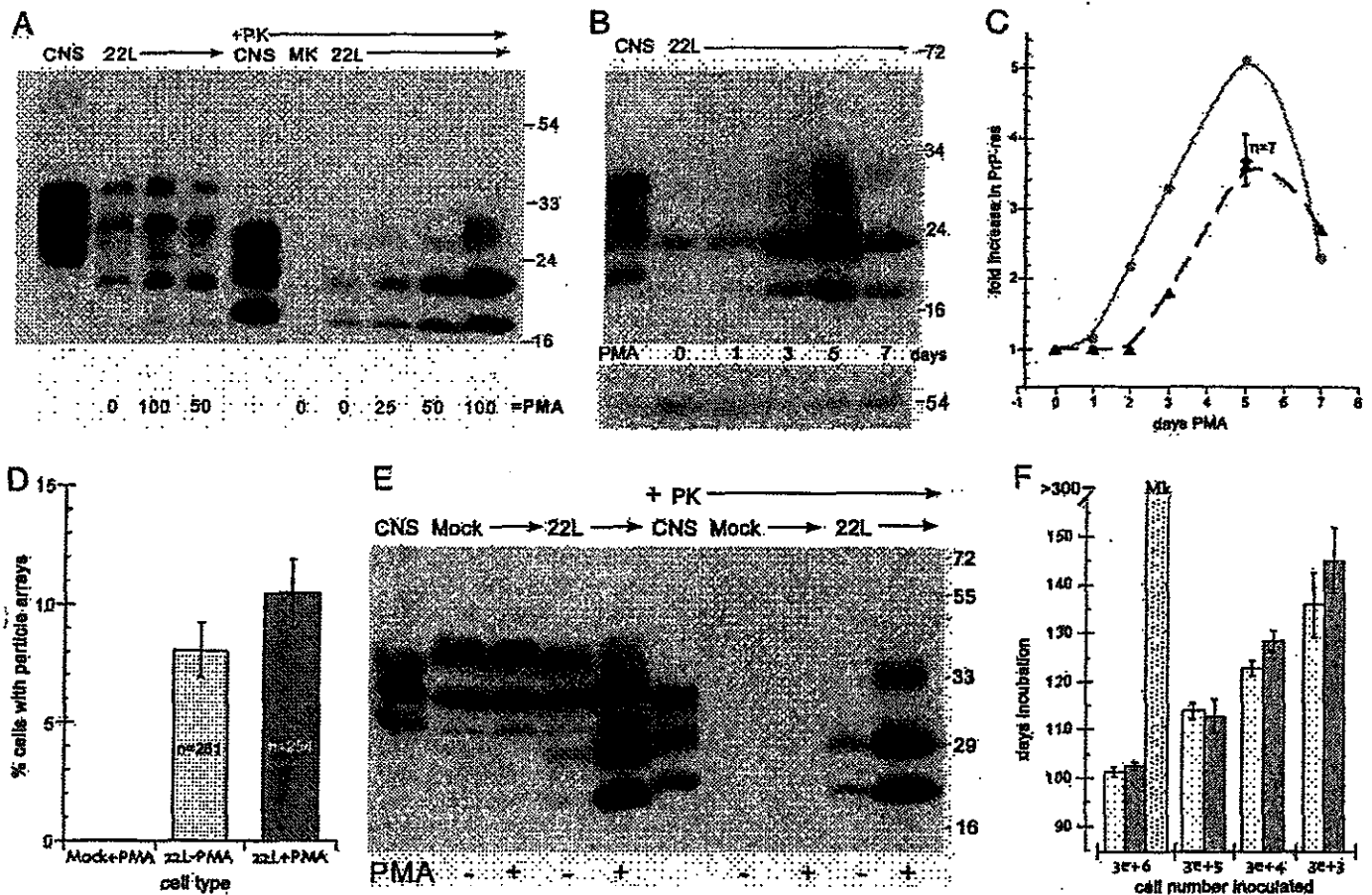


**Fig. 1.** Representative virus-like arrays of 25-nm particles in N2a + 22L (A–C) and in GT+FU-CJD (D) cells. (A and B) Particles in healthy cells treated with 100 ng/ml PMA for 5 days when PrP-res was markedly increased, with higher magnifications of the same array (Right). (C) From an N2a + 22L culture without PMA, processed in parallel. (D) A comparable virus-like array in a GT+FU-CJD cell. (A Left) The membrane-bound array is distant from the nucleus (N) and sits between a mitochondrion (m) and a vacuole (V). A 100-nm-diameter IAP retroviral is seen in an RER cistern (arrow), and Golgi membranes are at g. Arrows in the corresponding magnified image point to spherical dense particles of ~25 nm; note regions of variable compaction of particles. (B) A characteristic cluster of IAP retroviruses is seen to the right of a vacuole (V) in addition to a TSE-packed particle array adjacent to an isolated IAP (arrow). Higher magnification shows that the paracrystalline particles have sharper outlines than adjacent ribosomes. (C) Without PMA, spherical 25-nm particles also line up in an orthogonal pattern in more compact regions of N2a + 22L cells. (D) Orthogonal or paracrystalline arrangement of equivalent dense 25-nm particles in cross-section (e.g., at arrows) in infected GT cells that produce no retroviral structures is shown; a few similar 25-nm particles are seen in an adjacent swollen RER cistern (arrowhead), and these may represent a different stage of array development (see Results). (Scale bars: 100 nm.)



**Fig. 2.** Relationship of PrP-res, virus-like particles, and infectivity in N2a + 22L cells grown with and without PMA. (A) Dose-response from 0 to 100 ng/ml PMA for 5 days of PrP and corresponding PrP-res amounts (+PK lanes of whole-cell lysates treated with proteinase K as described in ref. 4). Note the strong increase in PrP-res at 100 ng/ml. CNS is brain homogenate control. MK are mock-infected cells and show no PrP-res. (B) PrP-res during continuous treatment with 100 ng/ml for 1–7 days shows the strongest response at 5 days; cells were treated in parallel and collected at sequential times. (C) Quantitative analysis of the increase in PrP-res in seven independent experiments with 75–100 ng/ml PMA (dotted line). Note the reproducible rise at 5 days ( $\pm$  SEM). The gray line shows the PMA-induced PrP-res increase versus a parallel nondrug control (see E) in cells that were tested for infectivity. (D) Count of virus-like 25-nm particle arrays in PMA-treated mock (uninfected N2a) control cells and in N2a + 22L cells without (22L-PMA) and with (22L+PMA) the drug. More than 250 cells were counted by EM for each sample, and the inclusion of any questionably positive arrays makes the percentage of positives overestimated. Nevertheless, there is no significant increase in the number of particle arrays with PMA. (E) Western blot of an aliquot of the mock-infected, untreated 22L, and PMA-treated 22L cells inoculated in mice for infectivity titrations. The mock cells show no PrP-res (+PK lanes), and the PMA-treated cells show an obvious increase in both PrP and PrP-res compared with their untreated counterparts. All cell lanes loaded with equal amounts of protein and infected CNS show brain-specific pattern (4). (F) Incubation time after inoculation of serial dilutions of N2a + 22L cell homogenates grown without PMA (white bars) and with PMA (gray bars). A shorter incubation time indicates a higher infectious titer. Mock-infected cells (dotted bar) at high concentrations elicited no clinical signs or neuropathology.

abnormal PrP *in situ* and/or infection also could be evaluated. The following report demonstrates 25-nm virus-like arrays in two cell lines productively infected with either sheep-derived scrapie or human-derived CJD agents passaged in mice. Comparable particles were not found in uninfected controls. These data, along with other drug and PrP immunogold binding studies here, lend further credence to the actuality of a TSE virion that is structurally independent of pathological PrP in the intact cell.

### Results

We examined two different types of infected cells in detail. These represented two different types of TSE agent, a sheep-derived scrapie strain known as 22L and a mouse-passaged human CJD agent designated FU. The FU-CJD agent is an Asiatic isolate that is much more virulent in mice than the standard sporadic CJD agents isolated from patients in the Western hemisphere (6). Each of these TSE strains was propagated in different cell types. The 22L scrapie strain was propagated in neuroblastoma N2a58 cells (designated N2a + 22L) whereas the hypothalamic

GT cell line was infected with FU-CJD (designated GT+FU-CJD). Thus, cell-specific and agent strain-specific influences could be monitored. Both infected cell types show abundant PrP amyloid fibrils by *in situ* immunocytochemistry (4) as well as high levels of PrP-res by Western blotting. As shown below, only the N2a cells (both uninfected and infected) produce endogenous intracisternal A type retroviral particles (IAPs). Thus, one could determine additionally whether these retroviral nucleic acid-protein complexes were linked to the production of 25-nm virus-like particles *in situ*. This was of interest because detergent-resistant IAP cores cosediment with TSE agents during subcellular fractionation of brain (18).

We initially searched for individual 25-nm dense round particles in regions of rough endoplasmic reticulum (RER) that had many developing IAPs and also looked for them in cytoplasmic regions with abundant PrP amyloid fibrils. Instead, we found dense virus-like 25-nm particles in paracrystalline arrays that were surrounded by a membrane. These bodies were separated from and morphologically different from both IAP clusters and